Spray formation from wall impingement-type atomizer

Inamura T.[1], Daikoku M.[2]

1. Faculty of Science and Technology, Hirosaki University, 3 Bunkyo-cho, Hirosaki-shi, Aomori-ken, Japan 036-8561
2. Department of Mechanical Systems on Information Technology, Hachinohe Institute of Technology, 88-1 Ohbiraki Myo, Hachinohe-shi, Aomori-ken, Japan 031-8501

The liquid film flow on a solid wall generated by the impingement of a liquid jet onto a solid wall has been analyzed theoretically using the laminar boundary layer model. The biquadratic velocity profile was employed for a laminar boundary layer, and it was assumed that the streamline radiates in all directions from the stagnation point on the wall. A gap between the centerline of a liquid jet and the streamline in a liquid jet, which passes through a stagnation point was assumed. The film thickness at the wall edge was measured by the contact needle method. From the measurements, the film thickness has a peak in the plane that intersects perpendicularly the solid wall surface and includes the liquid jet centerline. The film thickness decreases toward the peripheral, and then increases along the wall edge. The theoretical analysis of the film thickness on the wall agrees well with the measurements. The droplet sizes were measured by PDPA. The mean droplet size decreases toward the spray peripheral, and then increases. As the liquid injection pressure increases, the mean droplet size decreases.

1. Introduction

The wall impingement-type atomizer has some advantages. Since the thin liquid film on the solid wall can be obtained at relatively low liquid injection pressure compared to the other prefilming-type atomizer, the fine spray is generated easily. The spray configuration can be controlled by the shape of an impinged solid wall surface and impingement conditions. The deep penetration of a spray tip is obtained while keeping the liquid impingement velocity high. These advantages are very important for the combustor with high specific combustion load. On the other hand, this type atomizer has a disadvantage that the liquid deposits easily at the atomizer tip. To make clear these features of this type atomizer, the film flow on a solid wall and the disintegration mechanism of a liquid film should be understood.

The liquid film flow on a solid wall has been analyzed theoretically with reference to the film cooling. Watson[1] analyzed the liquid film flow using the theory of a laminar boundary layer. He obtained the velocity profile in the laminar boundary layer by integrating the momentum equation. Ishigai et al.[2] and Azuma et al.[3] analyzed the film flow using the assumption of the velocity profile in a laminar boundary layer. They studied the case of normal impingement of a liquid jet on the solid wall. In many cases of practical use of an impingement-type atomization, the oblique impingement will be employed. However, there are few studies on the film flow generated by the oblique impingement of a liquid jet on the solid wall.

In this paper the liquid film flow on the solid wall generated by the oblique impingement was studied theoretically and experimentally. The spray characteristics generated by the disintegration of a free liquid film issued from a solid wall edge were measured and were compared to the theoretical analysis.

2. Experimental apparatus

The experimental apparatus is shown in Fig.1. Liquid is fed from the water tank, which is pressurized by the compressed air from the compressor, to the liquid nozzle. The nozzle is mounted on the holder that is free of rotation. The solid wall on which the liquid jet impinges is free of parallel move. The liquid film and the spray issued from the solid wall edge were observed by the instantaneous photographs that were taken using the stroboscope and digital camera. The spray characteristics were measured by PDPA (30mW He-Ne, TSI Co.). The measurement point was located at 50mm downstream from the wall edge. The film thickness was measured by the contact needle method[4].

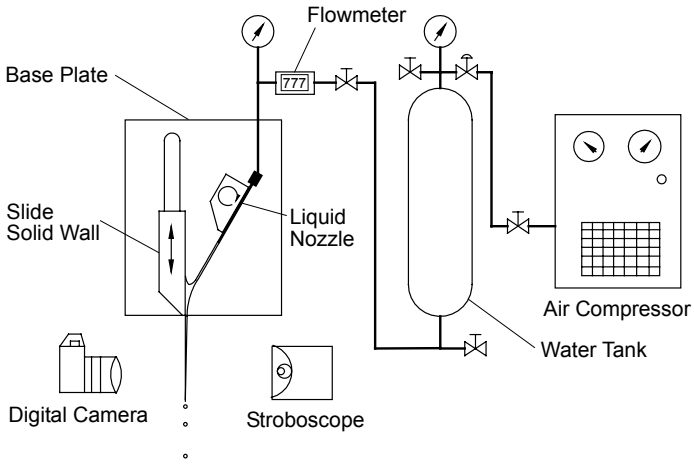

Fig.1 Experimental apparatus

In this paper the tap water was used as the atomized liquid. The impingement angle, θ that indicates the angle between the centerline of a liquid jet and the solid wall surface, is 30, 45 and 60deg. The range of a jet Reynolds number, $Re_j(=dU_0/\nu_l)$ was varied from 3000 to 10000. The distance between the liquid nozzle tip and the impingement point was fixed at 10mm. The distance between the impingement point and the solid wall edge, L was varied from 1 to 7mm. The inner diameter of a liquid nozzle, d (=2a) is 0.5 and 0.9mm. The length of both nozzles is 30mm.

3. Theoretical analysis of liquid film flow

In the case of the oblique impingement of a liquid jet on the solid wall, the liquid film flow on the solid wall was theoretically analyzed. Prior to the analysis, the following assumptions were made.

(1) The liquid flow is two-dimensional.
(2) The velocity distribution across the liquid jet is uniform and the liquid flows inside the liquid jet and the liquid film on the solid wall are laminar.
(3) On the solid wall, the laminar boundary layer develops in the liquid film from the stagnation point.
(4) The velocity distribution across a laminar boundary layer can be approximated by the biquadratic equation of Ishigai et al.[2];
(5) The liquid flowing in a minute angle dα in the liquid jet flows in a minute angle dϕ in the liquid film as shown in Fig.3. Where, the following geometric relationship of Rubel[5] exists between α,ϕ and θ ;

$$\tan\phi = \sin\theta \cdot \tan\alpha \tag{1}$$

(6) In the liquid jet, the distance between the center line of a jet and the streamline passing a stagnation point on the solid wall is expressed by the following equation[6];

$$\varepsilon\, a = a\cos\theta \tag{2}$$

(7) The effect of the airflow on the liquid film and that of the gravity on the film behavior can be ignored.

The symbols and the coordinate system used in the theoretical analysis are shown in Fig. 2. As shown in the figure, in the case of oblique impingement at the intersection point, O_1 between the centerline of a jet and the solid wall disagrees with the stagnation point, P_1.

The momentum equation of a laminar boundary layer is expressed generally by the following equation using the cylindrical coordinate;

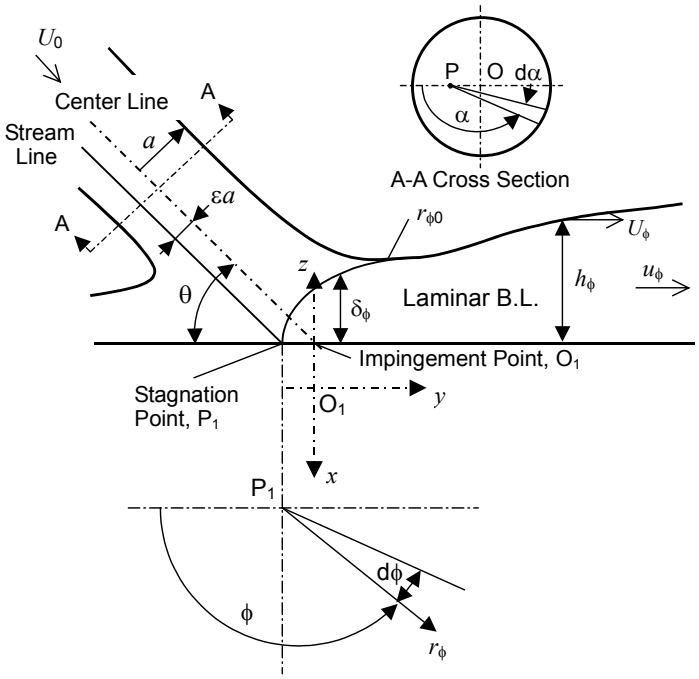

Fig.2 Coordinate system

$$\left(\frac{d}{dr}+\frac{1}{r}\right)\int_0^{\delta} u\left(U_0-u\right)dz=\nu_l\left(\frac{\partial u}{\partial z}\right)_{z=0} \qquad (3)$$

The film flow is classified using the point (r_ϕ=$r_{\phi 0}$) where the laminar boundary layer reaches the film surface.

(i) In the case that r_ϕ<$r_{\phi 0}$;

The velocity distribution across the laminar boundary layer is expressed by the assumption (4).

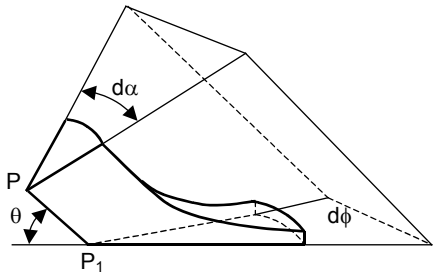

Fig.3 Liquid flow

$$u_\phi = U_0\left(2\eta_1 - 2\eta_1^{\,3} + \eta_1^{\,4}\right) \qquad (4)$$

where, $\eta_1 = z/\delta_\phi$ and δ indicates the laminar boundary layer thickness.

The substitution of Eq.(4) for Eq.(3) deduces the following equation;

$$\delta_\phi^{\,*} = 5.97\sqrt{r_\phi^{\,*}} \qquad (5)$$

where,

$$r_\phi^{\,*} = \frac{r_\phi}{a}\cdot\frac{1}{\mathrm{Re}^{1/3}} \qquad (6)$$

$$\delta_\phi^{\,*} = \frac{\delta_\phi}{a}\cdot\mathrm{Re}^{1/3} \qquad (7)$$

$$\mathrm{Re} = \frac{Q}{a\nu_l} \qquad (8)$$

The continuity condition at r_ϕ=$r_{\phi 0}$ and the assumption (5) deduce the following equation;

$$r_{\phi 0}^{\,*} = \frac{0.564}{(4\pi)^{1/3}}A^{2/3}B^{4/3} \qquad (9)$$

where,

$$A = \frac{\sin\theta}{\sin^2\phi + \cos^2\phi \cdot \sin^2\theta} \tag{10}$$

$$B = \pm\varepsilon\sqrt{\frac{\sin^2\theta}{\tan^2\phi + \sin^2\theta}} + \sqrt{1 - \frac{\varepsilon^2\tan^2\phi}{\tan^2\phi + \sin^2\theta}} \tag{11}$$

where, a sign of the first term in the right side of Eq.(11) is negative when 0<α<90deg., and positive when 90<α<180deg.
The continuity equation deduces the following equation of the film thickness;

$$h_\phi^* = \frac{1}{2r_\phi^*} A \cdot B^2 + 1.79\sqrt{r_\phi^*} \tag{12}$$

where,

$$h_\phi^* = \frac{h_\phi}{a}\mathrm{Re}^{1/3} \tag{13}$$

(ii) In the case that $r_\phi > r_{\phi 0}$;
The velocity distribution across the laminar boundary layer is expressed by the following equation;

$$u_\phi = U_\phi\left(2\eta_2 - 2\eta_2^{\,3} + \eta_2^{\,4}\right) \tag{4'}$$

where, $\eta_2 = z/h_\phi$
The substitution of Eq.(4)' for Eq.(3), the continuity condition at $r_\phi = r_{\phi 0}$ and the assumption (5) deduce the following equation;

$$h_\phi^* = \frac{0.642}{r_\phi^*} A \cdot B^2 + \frac{5.03\,r_\phi^{*2}}{A \cdot B^2} \tag{14}$$

The velocity of the liquid film surface is expressed by the following equation;

$$\frac{U_\phi}{U_0} = \frac{1}{0.899 + 7.04A^{-2}B^{-4}r_\phi^{*3}} \tag{15}$$

According to the analysis of the liquid film breakup by Fraser et al.[7] and Dombrowski and Hooper[8], the following equation of Sauter mean diameter was proposed in the present paper.

$$d_{32} = 1.08 \cdot d_L\left[1 + 3\mathrm{Oh}_l\right]^{1/6} \tag{16}$$

d_L indicates the liquid stem diameter that is calculated by the liquid film thickness and velocity at the wall edge[8]. The film thickness and velocity at the wall edge are calculated by using Eqs.(12), (14) and (15). Oh_l indicates the Ohnesorge number[8]. The correlation factor, 1.08 on the right hand side of Eq.(16) was determined by comparing the mean diameter with the measurements. Dombrowski and Hooper[8] recommended 1.19 as the correlation factor that is slightly larger than 1.08 of the present paper.

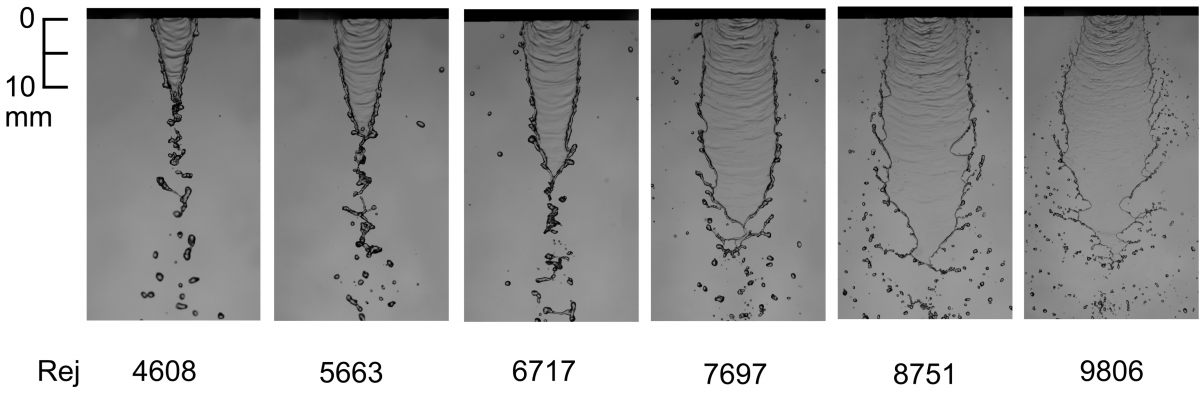

Fig.4 Breakup phenomena of liquid sheet (d=0.9mm, θ=30deg., L=3mm)

4. Results and discussions

4.1. Breakup phenomena and length of liquid film

The breakup phenomena of a liquid film issued from the solid wall edge are shown in Fig.4 that were taken varying the jet Reynolds number. The impingement angle was fixed to 30deg. The liquid film penetrates deeper and the droplets become smaller, as the jet Reynolds number increases.

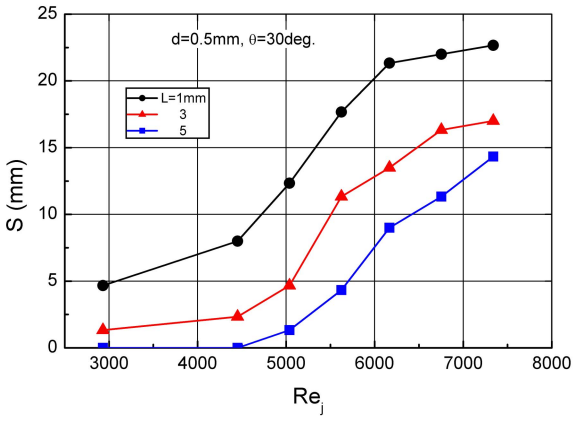

Fig.5 Breakup length

Figure 5 shows the breakup length of a liquid film, S as a function of the jet Reynolds number. The breakup length increases monotonically with the increase of the jet Reynolds number. At large Reynolds number, the breakup length seems to approach constant value in the present experimental range.

4.2. Liquid film thickness

The measurements of film thickness and droplet size were conducted using a liquid nozzle with the inner diameter of 0.5mm. Figure 6 shows the measured film thickness distribution compared to the calculation for three impingement angles. The film thickness that has a peak at the center decreases toward the periphery, and then increases rapidly. It has a minimum value at around x=2mm. As the impingement angle increases the distribution becomes flat one. Its peak diminishes, but the minimum value stays unchanged with the increase of the impingement angle. Figure 7 shows the film thickness distribution at various downstream locations from the impingement point. The distribution becomes flat one as the measurement point goes downstream. The peak diminishes and the minimum value increases toward downstream. At x=5mm, the measurements show quite larger values than the calculations. This is due to the hydraulic jump that was not taken account in the theoretical analysis. The measurements are almost coincident with the calculations except at x=5mm.

The peak film thicknesses at the center are shown in Figs.8 and 9 as a function of the jet Reynolds number and the distance between the impingement point and the measurement point, respectively. The film thickness decreases monotonically as the jet Reynolds number increases and as the distance increases. The calculations agree well with the measurements.

Figure 10 shows the calculations of the average film velocity. The average velocity decreases rapidly toward the periphery. The distance between the impingement point and the

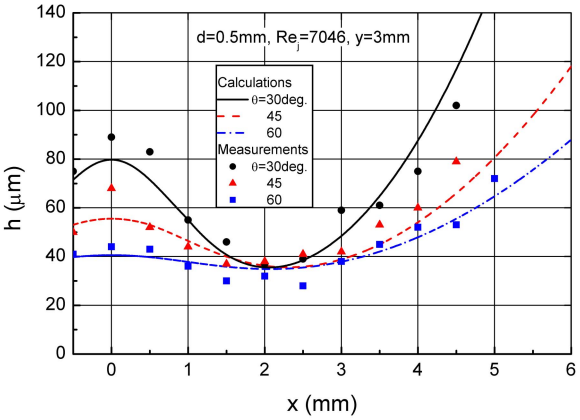

Fig.6 Film thickness distribution

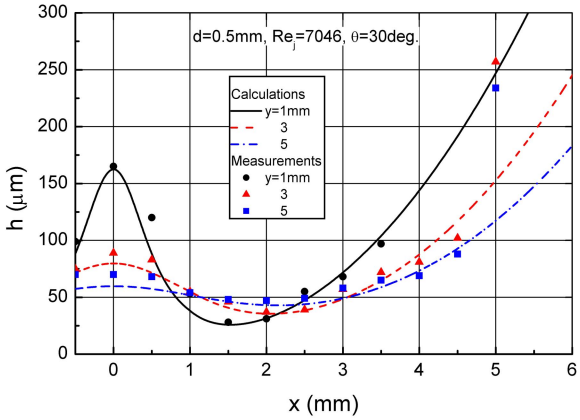

Fig.7 Film thickness distribution

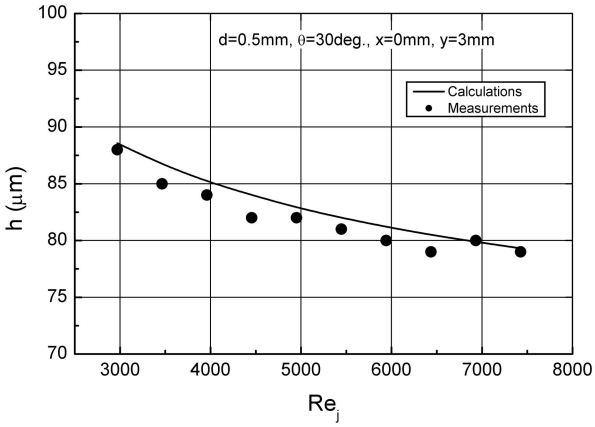

Fig.8 Influences of jet Reynolds number

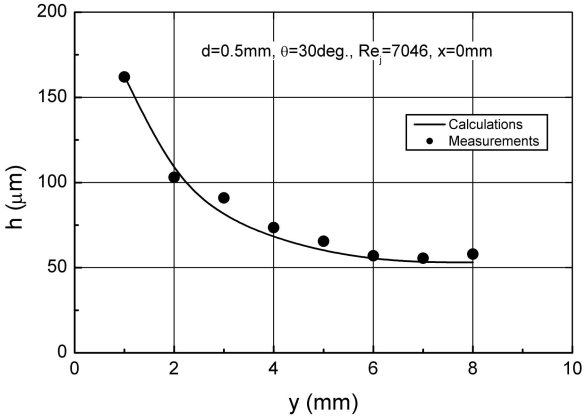

Fig.9 Influences of downstream location

measurement point increases, the peak lowers and the distribution approaches a flat one. Since the film thickness and the film velocity are important factors for the spray droplet size, it is inferred that the droplet size decreases rapidly as the liquid injection velocity increases.

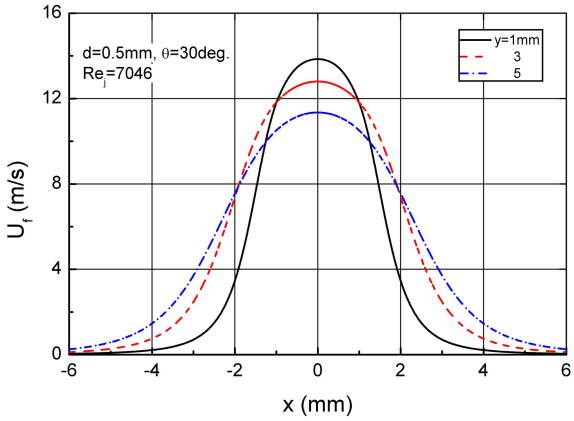

Fig.10 Average film velocity distribution

4.3. Spray characteristics

The Sauter mean diameter and droplet velocity were measured by the PDPA at 50mm downstream from the wall edge. Figure 11 shows the coordinate system for spray characteristics measurements.

Figure 12 compares the measurements of Sauter mean diameter, D with the calculations. The calculated mean diameters show almost constant values in the range of X=0 to 20mm at θ=45 and 60deg. The film thickness has a peak at the center and decreases toward the periphery as shown in Figs.6 and 7. On the other hand, the film velocity at the wall edge has a peak at the center and decreases rapidly toward the periphery as shown in Fig.10. The decrease of a film thickness decreases the droplet diameter and the decrease of a film velocity increases the droplet diameter. These two effects make the mean diameter constant. In the range of X=0 to 20mm, the effect of the impingement angle on the mean diameter is small. At θ=30deg. the

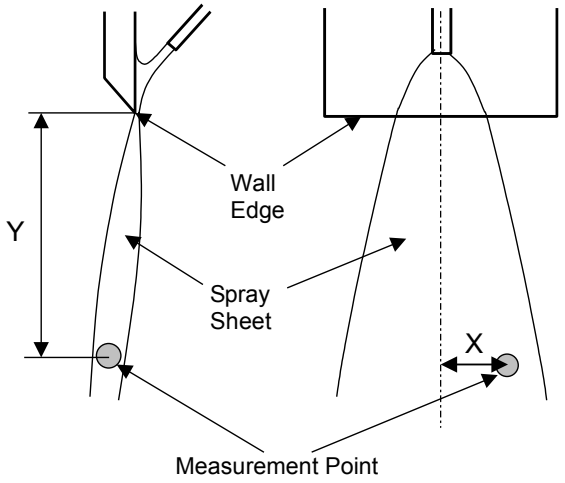

Fig.11 Coordinate System

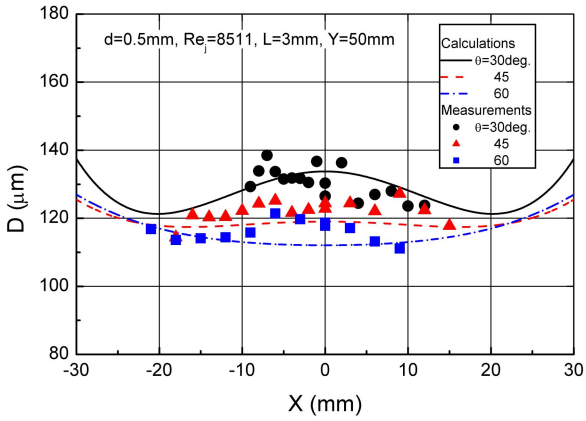

Fig.12 Mean diameter distribution

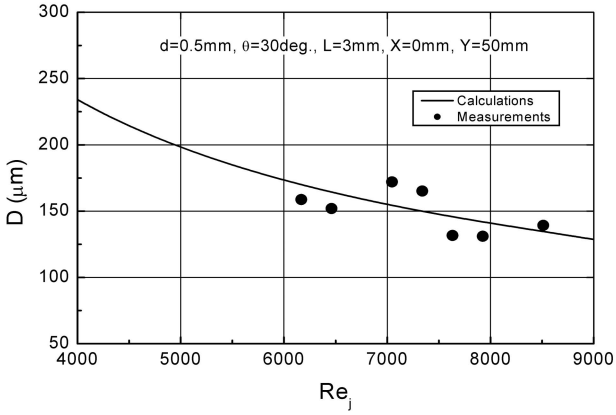

Fig.13 Effect of jet Reynolds number

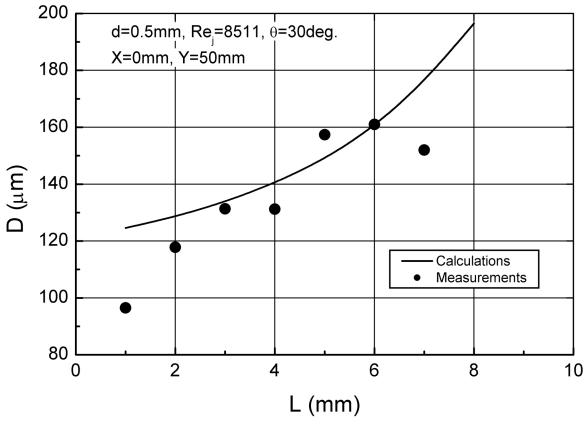

Fig.14 Effect of downstream location

mean diameter decreases, and increases toward the periphery. This trend is similar to that of the film thickness.

Figure 13 shows the effects of the jet Reynolds number on the Sauter mean diameter at the center. The mean diameter decreases rapidly as the jet Reynolds number increases. This is because that the film thickness decreases and the average film velocity increases as the Reynolds number increases.

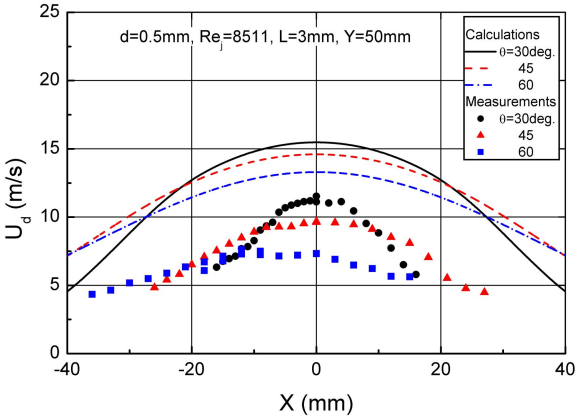

Fig.15 Average droplet velocity distribution

Figure 14 shows the effects of the distance between the impingement point and the wall edge on the mean diameter. The mean diameter increases with the distance. The film thickness decreases with the distance, however, the average film velocity at the wall edge decreases as the distance increases. In the present conditions, since the effect of the film velocity on the mean diameter is larger than that of the film thickness the mean diameter increases with the distance between the impingement point and the wall edge.

Figure 15 shows the Y-component distribution of an average droplet velocity at Y=50mm. In the calculations, it was assumed that the increase of the surface energy equals to the decrease of the liquid kinetic energy at the droplet formation and a droplet keeps an initial velocity at

the formation along its trajectory. The average droplet velocity decreases monotonically toward the periphery. Its distribution becomes the flat one as the impingement angle increases. The effects of the impingement angle on the average droplet velocity distribution by measurements are consistent qualitatively with those by calculations. However, the measured droplet velocities show rather smaller values than the calculations. These discrepancies mean that the liquid film and droplets are decelerated rapidly due to the surrounding air after they leave the wall edge.

5. Conclusions

The liquid film flow on the wall generated by the impingement of a liquid jet on the solid wall was investigated theoretically and experimentally. The film flow on the wall was analyzed theoretically using the laminar boundary layer model. The film thicknesses on the wall were measured by the contact needle method. In spite of several assumptions were made in theoretical analysis, the calculations of the film thickness by theoretical analysis agreed well with the measurements except at the peripheral of a liquid film. At the peripheral the discrepancies of the film thickness between the calculations and the measurements are due to the occurrence of a hydraulic jump that was not taken account in the theory.
The mean droplet sizes of the spray injected from the wall edge were predicted by using the liquid film breakup model proposed by Fraser et al. and the present theoretical analysis of a film flow on the wall. The correlation factor in the prediction equation of the mean droplet size was determined by the comparisons with the measurements. The correlation factor proposed in the present paper is slightly smaller than that recommended by Dombrowski and Hooper. The calculations and measurements of the mean droplet size showed almost constant values at the center part of the spray. The film thickness has a peak at the center and decreases toward the periphery. On the other hand, the film velocity at the wall edge has a peak at the center and decreases rapidly toward the periphery. The decrease of a film thickness decreases the droplet diameter and the decrease of a film velocity increases the droplet diameter. These two effects make the mean diameter constant. The predictions of the mean droplet size showed the good agreement with the measurements.

Acknowledgement

The authors would like to thank Mr. H. Furudate of Hachinohe Institute of Technology, Mr. F. Sato and T. Saito of Hirosaki University for their useful helps during the experiments.

6. References

[1] Watson E J 1964 *J. Fluid Mech.* **20** 481-499
[2] Ishigai K, Nakanishi S, Mizuno M and Imamura T 1976 *Trans. Japan Society of Mechanical Engineers (Ser.2)* **42** 1502-1510 (in Japanese)
[3] Azuma T and Wakimoto T 1997 *Proc. ICLASS-97* 70-77
[4] Tokuoka N and Sato G 1977 *Trans. JSME* **43** 3444-3454 (in Japanese)
[5] Rubel A 1981 *AIAA J.* **19** 863-871
[6] Hasson D and Peck R E 1964 *AIChE J.* **10** 752-754
[7] Fraser R P, Eisenklam P, Dombrowski N and Hasson D 1962 *AIChE J.* **8** 672-680
[8] Dombrowski N and Hooper P C 1962 *Chem. Eng. Sci.* **17** 291-305